Bread baking modeling: Coupling heat transfer and weight loss by the introduction of an explicit vaporization term

Davide Papasidero, Flavio Manenti *, Sauro Pierucci

Politecnico di Milano, Dipartimento di Chimica, Materiali e Ingegneria Chimica "Giulio Natta", Piazza Leonardo Da Vinci, 32, 20133 Milano, Italy

Received 16 July 2014
Received in revised form 15 September 2014
Accepted 21 September 2014
Available online 30 September 2014

1. Introduction and scopes

Food modeling is deserving increasing attention both from the scientific community and from the industrial world. Bread making consists of several phases (Della Valle et al., 2014), but when dealing with bread models, the most investigated one is certainly the baking phase. In this context, various assumptions can be made and several phenomena can be taken into account at different detail degree. Among these, water vaporization has rarely been described explicitly. The few authors that considered explicit formulation rates, used water vapor concentration dependent rates (Ousegui et al., 2010) based on the hypothesis of non-equilibrium evaporation in porous hygroscopic solids (Halder et al., 2011). This formulation (Eq. (1)) has two main problems: first, it needs the definition of a material and process-dependent parameter, not easy to estimate. Second, in the original dissertation (Scarpa and Milano, 2002), it is specified that a linear relationship between the evaporative flux and the vapor density difference is valid only in the case of small departure from the hygrometric equilibrium:

$$I_v = K(\rho_{v,eq} - \rho_v)S\varepsilon \tag{1}$$

In addition, even though considering the impact of the evaporation term into the energy balance (multiplying it by the latent heat of vaporization), the temperature "plateau" at 100 ° C is rather described by using effective thermal properties (Ousegui et al., 2010). A different approach that seems to be more physical does not consider explicit formulation of evapora-tion rate (Zhang and Datta, 2006; Nicolas et al., 2014), choosing to describe water vapor and liquid water as a unique moisture variable. In that case, the evaporation term is avoided in the water mass balance, but not in the energy one: it is then substi-tuted inserting the equation for liquid water or vapor, generating a dependence of the thermal balance from different partial derivatives.

Thus, it is a main aim of this paper to propose a different explicit vaporization term, fully coupling energy and mass balances. This formulation does not require to define a process-dependent parameter, better describing the physical problem of water vaporization inside bread during baking. Another aim of the current paper is that of using thermal properties depending on the macro-component mixture. This is another uncommon trend in bread baking modeling, especially considering properties varying with both temperature and composition. This can be useful for further studies on chemical kinetics applied on bread and, more generally, food cooking, as well as to take into account possible properties variation with food kind and chemical composition (e.g. viscoelastic properties).

* Corresponding author. Tel.: +39 02 2399 3273; fax: +39 02 7063 8173.
E-mail address: flavio.manenti@polimi.it (F. Manenti).

Nomenclature

A	pre-exponential factor for gas binary diffusivity
C_j	compound mass concentration per mixture unit volume, kg/m^3
C_p	heat capacity, kJ/kg/K
$C_{p,j}$	compound heat capacity, kJ/kg/K
D_w^i	water diffusivity, ith phase, m^2/s
D_{cv}	standard binary diffusivity between vapor and CO_2, m^2/s
h	convective heat transfer coefficient, W/m^2/K
H_{ev}	water latent heat of vaporization, J/kg
I_v	vaporization rate, kg/m^3/s
k_c	concentration numerical step function parameter, kg/m^3
K_m	mass transfer coefficient, m/s
K	non-equilibrium evaporation constant
k_t	temperature numerical step function parameter, K
m	mass, kg
m_j	mass of the jth component, kg
M_j	atomic mass of the jth component, kg
$\mathbf{n}$	normal direction
n_j^i	mass flux of jth component, ith phase, kg/m^2/s
Nu	Nusselt number
p	pressure, Pa
Q	heat flux, W
R	universal gas constant, 8.314 J/mol/K
S	pore saturation
t	time, s
T	temperature, K
v	oven average air velocity
V	volume, m^3
V_j	volume of the jth component, m^3
$\tilde{V}_j$	molecular volume of jth gas component, m^3
W	moisture content, kg/kg
x, y, z	coordinates

Greek symbols

δ	differential operator
ε	porosity
κ	step function
λ	thermal conductivity, W/m/K
ρ	intrinsic density, kg/m^3
τ	oven temperature trend parameter, s
φ	volumetric fraction
ω	mass fraction

Subscript

ash	ash
C	with concentration
carb	carbohydrate
CO_2	carbon dioxide
env	oven environment
fat	fat
fiber	fiber
j	jth compound
prot	protein
start	oven initial
sp	set point
T	with temperature
w	water

Superscript

0	initial
CHOI	from the paper of Choi and Okos (1986)
eff	effective
eq	equilibrium
f	final
l	liquid
i	ith phase
v	vapor

To satisfy these aims, some idealities have been assumed, going to the detriment of model accuracy for specific cases. Anyway, further details can be added by refining the models for the related phenomena (e.g. considering convection in the energy balance, using specific thermal properties, taking volume expansion into consideration, etc.).

2. Materials and methods

The validation of the bread baking model needed to perform baking experiments for getting temperature vs. time data and weight loss measurements. The baking test was repeated three times, with a couple of analog cases and a third case with different initial weight for a sensitivity analysis. Since the experimental data are consistent between the series of experiments, only one configuration is presented and discussed in details.

2.1. Bread samples

Samples were prepared using a standard recipe for bread: wheat flour (100%), water (58%), salt (2% g), dry yeast (2%). The flour composition is (g per 100 g): carbohydrates (70.8), proteins (12.0), fats (1.5), fibers (3), water (12.7). Dough was made by mixing the ingredients manually, then underwent double leavening process for a total time of about 1 h at ambient temperature. The individual sample of about 810 g (shaped as an Italian "Pagnotta bread" – approximate oblate ellipsoid, ca. 0.217 m diameter 0,05 m height, see also Papasidero et al., 2014) was formed and placed on a grid covered by a piece of oven paper to hold the dough avoiding any drip on the oven base and minimizing the fluid dynamics and heat distribution effects of the support.

2.2. Baking tests

The domestic oven (KitchenAid, USA) was pre-heated to the set point temperature of 200 °C. Then, the grid with the sample was positioned in the central zone of the oven to achieve homogeneous air distribution. The sample was baked under forced convection (v = 2 m/s) for about 40 min, terminating when a golden-brown crust format on the bread. The temperature was measured all along the test in the oven and inside the bread, while weight was measured before and after the baking process.

3. Experimental results

3.1. Temperature

The temperature trend for the bread center and for the oven is reported in Fig. 1. From this it can be seen the oven temperature increase till the set point temperature is reached. The oven controls this parameter with ±5.7 °C accuracy, oscillating.

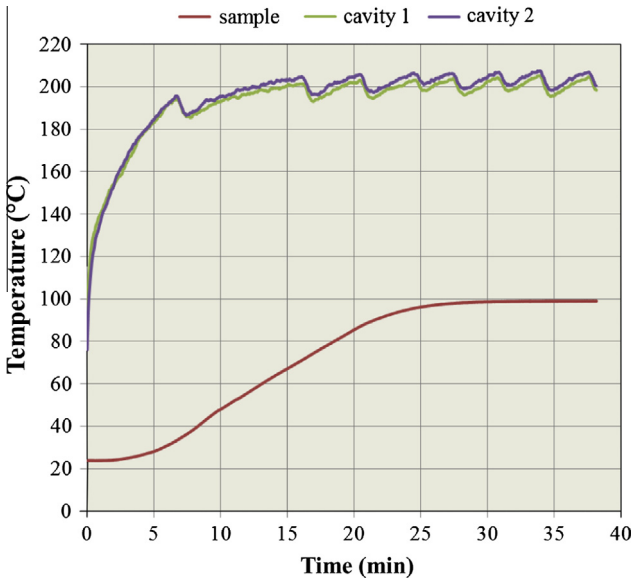

Fig. 1. Temperature profiles for oven (cavity) and bread core (sample).

Bread core temperature grow slowly in the first 5 min (lag phase due to thermal gradient not yet established), then a ramp-like growth can be seen in the next 20 min, until a plateau phase is reached at about 97–99 °C. This trend is yet seen in literature (Zhang and Datta, 2006; Nicolas et al., 2014).

It is worth to underline that the oven temperature starts from about 100 °C due to the door opening, then quickly raise back to 200 °C. In this sense, the main target of the experimentation is to analyze bread baking in a domestic oven. This can require pre-heating and door opening, not necessarily common in the industrial practice.

3.2. Weight and water loss

Baked bread weight measure (738 g) evidences a loss of about 72 g (8.9%) with respect to the initial dough mass (810 g). This is certainly due to the drying process, as expected and confirmed from literature (Purlis and Salvadori, 2009a).

3.3. Dimension increase

The bread diameter increases from 21.7 cm to 22.6 cm. The diameter measure is the average of 3 different diameters, with a difference of 0.4 cm between the maximum and the minimum one. The height increases from 5.0 to 7.0 cm. Then, the bread volume increase is about 51% of the original volume.

4. Mathematical model

4.1. Governing equations

The process variables during the baking process are liquid water mass fraction, vapor mass fraction and temperature. Other process variables, like volume, pressure, etc. are considered to be constant. Water vapor and CO_2 are assumed to be ideal gases. The resulting partial differential equation (PDE) system is built based on the conservation principles and takes into account an explicit formulation for the vaporization term, I_v, assuming a direct dependence on the heat flux and on the bread temperature. By doing this, one can identify three situations, based on the temperature reached in the media and related to water phase change:

- $T < 100$ °C. Vaporization by ebullition is not occurring. Water vapor production in the pores by evaporation is considered to be negligible and temperature rises due to the incoming heat flux.
- $T > 100$ °C., $C_w^l > 0$. When the boiling temperature is reached, it remains constant and the matter enters the ebullition regime. Liquid water turns into water vapor, until it finishes.
- $T > 100$ °C, $C_w^l = 0$. When liquid water is completely vaporized, the temperature starts to rise again, approaching the oven one.

It is possible to describe these phases by the introduction of two step functions, κ_T and κ_C. These functions (Figs. 2 and 3) are defined as follows:

$$\kappa_T = \begin{cases} 0 & \text{if } T < 100\,^{\circ}\text{C} \\ 1 & \text{if } T \geqslant 100\,^{\circ}\text{C} \end{cases} \tag{2}$$

$$\kappa_C = \begin{cases} 0 & \text{if } C_w^l = 0 \\ 1 & \text{if } C_w^l > 0 \end{cases} \tag{3}$$

All the balances include this function to manage the three cases, as shown below.

The vaporization term I_v is then defined as the vapor produced by the local heat flux when $T > 100$ °C and $C_w^l > 0$:

$$I_v = \frac{Q}{H_{ev}} \tag{4}$$

where H_{ev} represents the enthalpy of vaporization of water, and is assumed to have a constant value of 2272 J/kg, due to the constant pressure hypothesis.

It is worth to underline that water vapor production in the bread pores by evaporation at $T < 100$ °C is assumed to be negligible when compared to that produced by ebullition at $T > 100$ °C. A more detailed model would require this phenomena to be involved in the material and heat balances but, in this specific case and due to the different order of magnitude, the model results would not benefit from this phenomena inclusion.

In this way, the mass and energy balances, functions of the considered variables, can be written as follow.

4.1.1. Liquid water balance

$$\frac{\partial C_w^l}{\partial t} + \nabla \cdot \mathbf{n}_w^l = \kappa_T \kappa_C (-I_v) \tag{5}$$

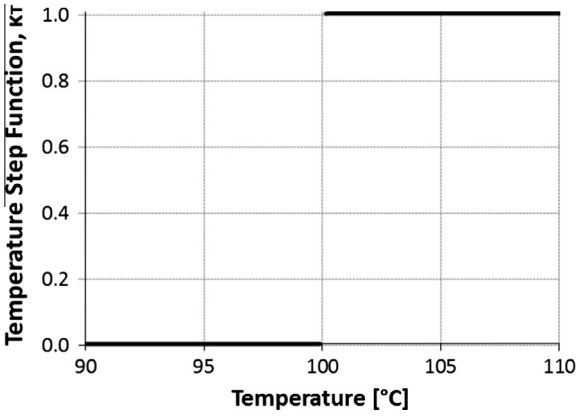

Fig. 2. Step function for boiling temperature.

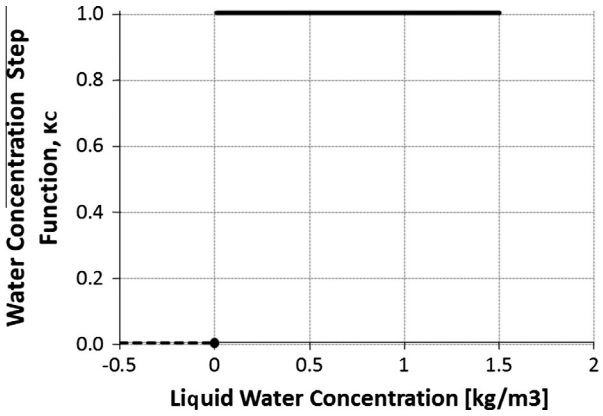

Fig. 3. Step function for concentration.

4.1.2. Water vapor balance

$$\frac{\partial C_w^v}{\partial t} + \nabla \cdot \mathbf{n}_w^v = \kappa_T \kappa_C I_v \tag{6}$$

4.1.3. Energy balance

$$\rho c_p \frac{\partial T}{\partial t} + \nabla \cdot (\lambda \nabla T) = \kappa_T \kappa_C I_v H_{eV} \tag{7}$$

Note that for temperatures higher than 100 °C ($\kappa_T = 1$) and in case the liquid water is still present ($\kappa_C = 1$), the heat flux Q, equal to the conduction flux ($\lambda \nabla T$) (plus the convection term, here neglected for simplification due to the different orders of magnitude), brings the energy balance to become:

$$\rho c_p \frac{\partial T}{\partial t} = 0 \tag{8}$$

representing the condition of constant temperature (“plateau”).

Since the pressure in the bread is considered to be constant, the liquid water and water vapor fluxes are not considered to belong to pressure gradients (as, for example, suggested by Zhang and Datta (2006))) or to temperature gradient (Nicolas et al., 2014). Thus, an effective diffusivity is introduced for the two fluxes, and a concentration dependence is set.

$$\mathbf{n}_w^l = D_w^l \nabla C_w^l \tag{9}$$
$$\mathbf{n}_w^v = D_w^v \nabla C_w^v \tag{10}$$

4.2. Initial and boundary conditions

4.2.1. Initial conditions

The initial temperature is the dough temperature, while the initial concentration for the liquid water is directly determined by the bread formulation. The initial water vapor concentration is set as 0 due to the related negligibility assumption (see Section 4.1):

$$\begin{cases} C_w^l = C_{w,0}^l \\ C_w^v = 0 \\ T = T_0 \end{cases} \tag{11}$$

4.2.2. Boundary conditions

The boundary condition for the energy balance takes into account the heat transfer by convection and radiation: an overall heat transfer coefficient is introduced due to the complexities that the rigorous dissertation requires. This permits to avoid the emissivity and view factors estimations, and to consider a homogeneous environment.

$$\mathbf{Q} \cdot \mathbf{n} = h(T - T_{ext}) \tag{12}$$

The free liquid water is assumed not to leave the surface of the bread (whereas different foodstuff can undergo dripping phenomena during the cooking process, e.g. meat (Dhall et al., 2012)).

$$\mathbf{n}_w^l \cdot \mathbf{n} = 0 \tag{13}$$

The water vapor leaves the surface due to concentration difference between the bulk and the bread surface:

$$\mathbf{n}_w^v \cdot \mathbf{n} = K_m (C_w^v - C_{w,ext}^v) \tag{14}$$

where K_m is an overall mass transfer coefficient in analogy with the thermal boundary condition, Eq. (12). The bulk concentration, function of the relative air humidity (environment RH% was about 71% at 25 °C), is considerably lower than the internal one. For this reason, it could be neglected in the calculations, while in other circumstances it could be useful to take into consideration, especially when dealing with steam ovens. Indeed, air humidity can be useful as a parameter for oven, cooking programs and recipes design and optimization (Schirmer et al., 2011).

4.3. Material properties

Due to the high non homogeneity of food systems, it is impossible, or at least very hard (Datta et al., 2012), to get the exact food material properties for a specific sample. For example, as two pieces of beef roast could have differences in fat content, two different breads could have a different formulation (different ingredients). For this reason, it is common to find modeling and simulation works where the material properties are tailored for the specific case. Once that a “standard sample” is decided, the assumptions on the food systems have to be defined: number of phases, homogenization (Quang et al., 2011), temperature dependence, mixing rules (in case of multi-component phases), etc. A good example in this sense is the work by Purlis and Salvadori (2009a,b), where the authors decided to model bread baking by using temperature dependent physical properties. They used effective properties for a homogenous media that not only vary with the model temperature, but also include the crumb-to-crust transition (and then, effectively, the water vaporization term for the energy balance) in the properties themselves, by the use of numerical Heaviside and Dirac functions.

A very different approach is the homogenization, where, according to Gulati and Datta (2013), a “porous media formulation homogenizes the real porous material and treats it as a continuum where the pore scale information is no longer available”. This approach, also taken into consideration by other research groups (e.g. (Nicolas et al., 2014)), considers the medium as a multiphase continuum, with material balances regarding some components in three phases: a “vapor phase”, usually bringing to mass balances on water vapor and, sometimes, CO_2, a “liquid water phase” and a “solid” component, chosen as an averaged bulk material (Jury et al., 2007). In the case of baked goods, the thermal properties for the solid phase are rarely based on composition functions of single component properties, while for other processes (e.g. fish drying, food frying, etc.), it can happen to find a solid phase made up of different components (Rahman et al., 2002; Williams and Mittal, 1999). Even in those cases, the thermal properties are often considered to be constant with temperature, and it is uncommon to run into mass balances that consider chemical reactions, result-ing in a global constant mass for them (with the exception of CO_2 production by fermentation).

The present work considers the use of well-known empirical correlations (Choi and Okos, 1986) for calculating effective properties for the bread (density, heat capacity and thermal conductivity), based both on composition and on the local temperature. This is an enormous advantage when considering reacting mixtures, which are the main reason for this choice: in fact, one of the aims of this work is to provide a model ready to be applied to cases where chemical reactions lead to substantial modifications to the sensorial profile, e.g. browning, starch gelatinization, CO_2 formation, etc. Macro-components, like proteins, carbohydrates, ashes, fibers, fats are considered for the solid phase, but this approach can be extended to more specific components.

An extensive review on property estimation equations for transport phenomena based models in food process engineering can be found in the paper by Gulati and Datta (2013). Some interesting review papers of the recent advances on baking processes and related simulation can be found in literature (Chhanwal et al., 2011; Purlis, 2012). A recent interesting paper on how to deduce material transport properties using a soft matter approach can be found in Datta et al. (2012).

4.3.1. Density

Density is involved both in the mass and in the energy balances. In this work, there is a difference between the intrinsic compound density and its concentration in the mixture. In fact, the former is the mass per unit volume of the pure compound (Eq. (15)), while the latter is the compound mass per unit volume of the mixture (Eq. (16)), and considers the medium as made of three phases, with a certain porosity and pore saturation. The total mass for each component can be therefore deduced by integrating the mass concentration in the total volume domain.

$$\rho_j = \frac{m_j}{V_j} \tag{15}$$

$$C_j = \frac{m_j}{V} \tag{16}$$

The intrinsic densities of the macro-components are described as polynomial functions of temperature, according to the following equations (N.B.: temperature is in °C for the equations from (17)–(21), whilst it is in K for Eqs. (23) and (24)):

$$\rho_{prot} = 1.3300 \times 10^3 - 0.5184T \tag{17}$$

$$\rho_{carb} = 1.5991 \times 10^2 - 0.31046T \tag{18}$$

$$\rho_{fat} = 9.2559 \times 10^2 - 0.41757T \tag{19}$$

$$\rho_{fiber} = 1.3115 \times 10^3 - 0.36589T \tag{20}$$

$$\rho_{ash} = 2.4328 \times 10^3 - 0.28063T \tag{21}$$

$$\rho_w^l = 9.9718 \times 10^2 + 3.1439 \times 10^{-3}T - 3.7574 \times 10^{-3}T^2 \tag{22}$$

$$\rho_w^v = \frac{P \cdot M_{H_2O}}{RT} \tag{23}$$

$$\rho_{CO_2} = \frac{P \cdot M_{CO_2}}{RT} \tag{24}$$

The related mixture density is calculated with a parallel model weighed on the mass fractions:

$$\rho = \frac{1}{\sum \frac{\omega_j}{\rho_j}} \tag{25}$$

4.3.2. Heat Capacity

Using a similar approach, heat capacity is first defined for the single components (Eqs. (26)–(33)) and then calculated using a mass fractions averaged mixing rule (Eq. (34)) (N.B.: temperature is expressed in °C for the equations from (26)–(31), whilst it is in K for Eqs. (32) and (33)):

$$C_{p,prot} = 2.0082 + 1.2089 \times 10^{-3}T - 1.3129 \times 10^{-6}T^2 \tag{26}$$

$$C_{p,carb} = 1.5488 + 1.9625 \times 10^{-3}T - 5.9399 \times 10^{-6}T^2 \tag{27}$$

$$C_{p,fat} = 1.9842 + 1.4733 \times 10^{-3}T - 4.8008 \times 10^{-6}T^2 \tag{28}$$

$$C_{p,fiber} = 1.8459 + 1.8306 \times 10^{-3}T - 4.6509 \times 10^{-6}T^2 \tag{29}$$

$$C_{p,ash} = 1.0926 + 1.8896 \times 10^{-3}T - 3.6817 \times 10^{-6}T^2 \tag{30}$$

$$C_{p,w}^l = 4.1762 + 9.0862 \times 10^{-5}T + 5.4731 \times 10^{-6}T^2 \tag{31}$$

$$\frac{C_{p,w}^v}{R} = 3.49708 + 1.5226033 \times 10^{-3}T + 2.2301684 \times 10^{-8}T^2 - 5.9706577 \times 10^{-11}T^3 \tag{32}$$

$$\frac{C_{p,CO_2}}{R} = 3.28677 + 5.1201479 \times 10^{-3}T + 2.2351997 \times 10^{-6}T^2 - 3.3521927 \times 10^{-10}T^3 \tag{33}$$

$$C_p = \sum C_{p,j}\omega_j \tag{34}$$

It is important to underline that the mass fraction is considered as a local property and not as a global one, in order to take into account the non-homogeneity of the final product (e.g. it is affected by the local temperature). In this sense, the definition can be deduced from the component mass of an infinitesimal, exploiting the abovementioned concentration definition, Eq. (16):

$$\omega_j = \frac{\delta m_j}{\delta m} = \frac{\delta m_j}{\sum \delta m_j} = \frac{C_j \delta V}{\sum C_j \delta V} = \frac{C_j}{\sum C_j} \tag{35}$$

4.4. Thermal conductivity

Thermal conductivity follows the abovementioned approach. The pounded weighed average on volume fractions, as defined by Choi and Okos (Eq. (36)), is assumed to be adequate for the conductivity estimation.

$$\lambda = \sum \lambda_j \varphi_j \tag{36}$$

Nonetheless, their estimated volume fraction formula (Eq. (37)), appeared to be wrong due to the fact that we are also including the gas phase species. Those species have a considerably low intrinsic density (i.e. very high specific volume) when related to liquid and solid compounds. This can lead to an abnormal trend for the volume fractions.

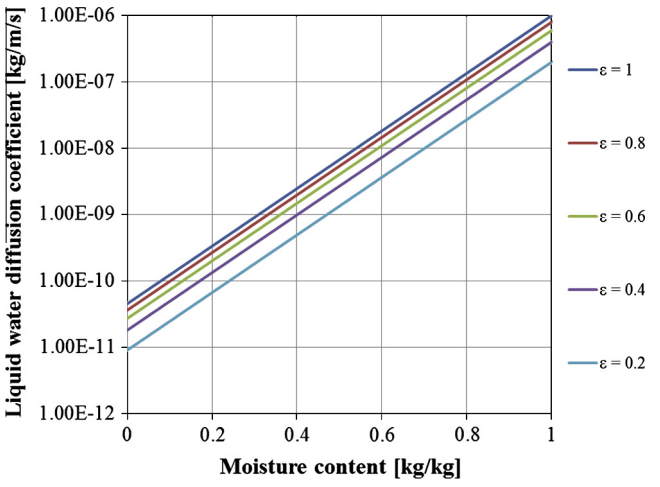

Fig. 4. Liquid water diffusion coefficient as a function of moisture content and porosity.

$$\varphi_j^{CHOI} = \frac{\frac{\omega_j}{\rho_j}}{\sum \frac{\omega_j}{\rho_j}} = \rho \frac{\omega_j}{\rho_j} \tag{37}$$

The appropriate formula for the volume fraction of the compounds can be deduced starting from the infinitesimal volumes and substituting the concentration and density definitions (respectively Eqs. (16) and (15)):

$$\varphi_j = \frac{\delta V_j}{\delta V} = \frac{\delta m_j}{\rho_j} \frac{1}{\delta V} = \frac{C_j \delta V}{\rho_j} \frac{1}{\delta V} = \frac{C_j}{\rho_j} \tag{38}$$

The components thermal conductivity is then calculated by using other polynomial expressions (N.B.: temperature is in °C for the equations from (39)–(44), whilst it is in K for Eqs. (45) and (46)):

$$\lambda_{prot} = 1.7881 \times 10^{-1} + 1.1958 \times 10^{-3} T - 2.7178 \times 10^{-6} T^2 \tag{39}$$

$$\lambda_{carb} = 2.014 \times 10^{-1} + 1.3874 \times 10^{-3} T - 4.3312 \times 10^{-6} T^2 \tag{40}$$

$$\lambda_{fat} = 1.8071 \times 10^{-1} - 2.7604 \times 10^{-3} T - 1.7749 \times 10^{-7} T^2 \tag{41}$$

$$\lambda_{fiber} = 1.8331 \times 10^{-1} + 1.2497 \times 10^{-3} T - 3.1683 \times 10^{-6} T^2 \tag{42}$$

$$\lambda_{ash} = 3.2962 \times 10^{-1} + 1.4011 \times 10^{-3} T - 2.9069 \times 10^{-6} T^2 \tag{43}$$

$$\lambda_w^l = 5.7109 \times 10^{-1} + 1.7625 \times 10^{-3} T - 6.7036 \times 10^{-6} T^2 \tag{44}$$

$$\lambda_w^v = 2.09915 \times 10^{-5} + 1.34528 \times 10^{-7} T \tag{45}$$

$$\lambda_{CO_2} = 4.066238 \times 10^{-6} + 7.1956 \times 10^{-8} T \tag{46}$$

4.4.1. Diffusivities

The most common formula for the liquid diffusion coefficient is a function of moisture content and porosity of the bread sample (Jury et al., 2007; Zhang and Datta, 2006):

$$D_w^l = 10^{-6} \exp(-10 + 10W)\varepsilon \tag{47}$$

It ranges from a value of 0 (in absence of pores) to the maximum asymptotic value of 10^{-6}, with high porosity and moisture content (Fig. 4).

A reasonable averaged constant value could range between 10^{-9} and 10^{-7}, and could be used as a parameter to fit the total moisture loss from experiments.

Water vapor diffuses faster than liquid water. A well-known correlation for the effective diffusivity of vapor has been introduced by Ni (1997), and correlate it to the standard diffusivity between vapor and CO_2, to the pore saturation and to the porosity, according to the following formula:

$$D_w^{v,eff} = D_{cv}((1 - 1.1S)\varepsilon)^{4/3} \tag{48}$$

This could be used for deriving the order of magnitude of the vapor diffusivity in CO_2.

According to the process temperature (about 20–200 °C), the obtained value for vapor is about 0.02–0.04 cm^2/s.

4.4.2. Free and bound water

The dry bread crust has a percentage of residue water, which can be associated to the bound water. This concept is adopted in food engineering to predict the final water content and to consider the fact that a certain quantity of water is physically bonded to the food matrix and it is difficult to remove.

For this reason, just a fraction of the total liquid water is assumed not to head to evaporation and diffusion. This fraction is chosen as a function of the final crust moisture content, whose value is taken from literature (Czuchajowska et al., 1989).

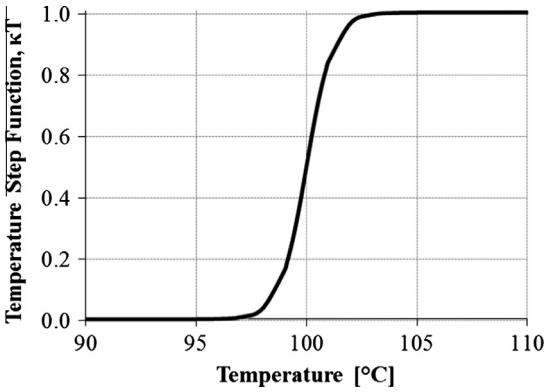

Fig. 5. Numerical step function for boiling temperature.

4.5. Numerical implementation

The presented PDE system has been implemented in a commercial FEM software that permits to solve PDE systems.

4.5.1. Numerical step functions

As described in Section 4.1, two step functions (Eqs. (2) and (3)) are introduced in the model to directly take into account the vaporization phenomena. Nonetheless, it would be impossible to solve the PDE system by using the original formulas. In fact, applying the spatial discretization and then Newton method based algorithms to solve the PDE system, the solver has to integrate the resulting ordinary differential equations (ODE) system for every time step. This presuppose the Jacobian to be calculable. In case of discontinuities, as for the analytical step functions (2) and (3), it is not possible to calculate the Jacobian in the discontinuity points, then the Newton method is not applicable. For this reason, a numerical (sigmoid-like) formulation for the step functions has been employed (Eqs. (49) and (50)), eliminating the discontinuities and permitting the calculation of the ODE system Jacobian.

$$\kappa_T^{num} = \frac{1}{(1 + \exp(-(T - T_{vap})/(k_T)))} \tag{49}$$

$$\kappa_C^{num} = \frac{1}{\left(1 + \exp\left(-\left(C_w^l - C_{shift}\right)/(k_C)\right)\right)}, \quad \text{with } C_w^l \geqslant 0 \tag{50}$$

As functions of the parameters k_T and k_C, these expressions are more or less smoothed (Figs. 5 and 6). The choice of those parameters strongly affects the numerical solution. C_{shift} parameter is introduced to permit the sigmoid to be effectively null at concentrations next to 0 and it is deduced iteratively. Even if the Jacobian

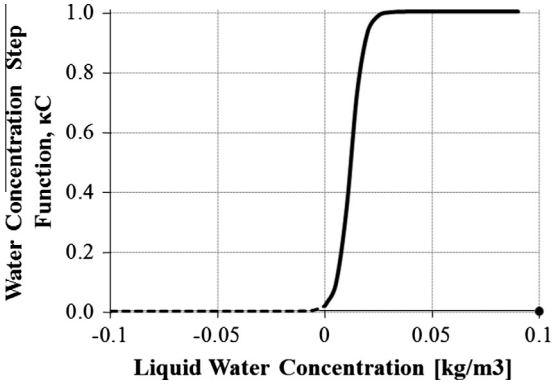

Fig. 6. Numerical step function for concentration.

Table 1
Model parameters.

Parameter	Description	Value
h	Heat exchange coefficient	20 W/m/K
k_{mat}	Material exchange coefficient	4.e−4 m/s
D_w^l	Liquid water diffusion coefficient	1.e−8 m^2/s
D_w^v	Water vapor diffusion coefficient	1.e−4 m^2/s
C_{shift}	Concentration shift numerical step function parameter	0.012 kg/m^3
k_T	Temperature numerical step function parameter	3 °C
k_C	Concentration numerical step function parameter	1.e−3 kg/m^3
τ	Oven temperature trend parameter	320 s

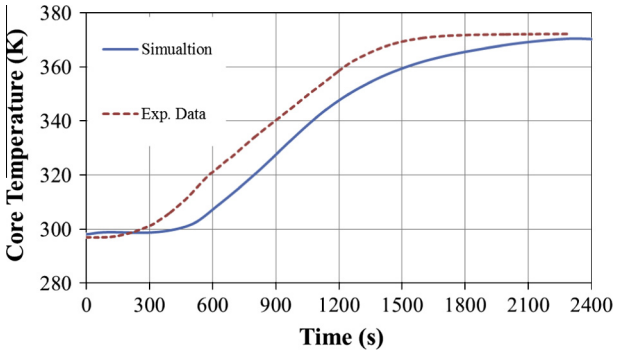

Fig. 7. Temperature trend. Model and experimental data comparison.

becomes calculable, it could have some matrix elements with very high values (due to almost-vertical trend and then to derivatives that tend to infinite), being almost numerically singular and bringing either to a need for a smaller time step or not working at all with the solver. If the maximum iteration number or the minimum time step is achieved, the model solution stops. The chosen values for the application case are reported in Table 1.

4.5.2. Oven temperature

The temperature trend in the oven, as discussed in Section 3, is that of a pre-heated oven. This trend is not constant due to the door opening for inserting the bread between the pre-heating and cooking phases. Then, it took about 10 min for achieving the set point temperature of 200 °C. Therefore, an exponential expression that tends to the set point temperature has been introduced (Eq. (51)). The parameters that describe the temperature trend are estimated from experimental data regression, and reported in Table 1.

$$T_{env} = T_{start} + (T_{sp} - T_{start})\left[1 - \exp\left(-\frac{t}{\tau}\right)\right] \tag{51}$$

T_{env} is the average oven temperature, T_{start} is the initial temperature after the insertion of the dough, T_{sp} is the set point temperature, and τ is a parameter that takes into account the temperature/time dependence. This expression is flexible enough to represent the temperature trend in case of cooking without pre-heating the oven chamber (Purlis and Salvadori, 2009b).

5. Results and discussion

The approach presented in Section 4 has been applied to model the experimental results from the presented test (Section 3). Based on the operating conditions, the authors deduced the model parameters that represent them. Those are reported in Table 1.

5.1. Bread temperature

Applying the model to the test case to simulate the bread core heating, the obtained results on temperature prevision (Fig. 7) seem to follow the experimental trends, despite a delay time of about 3 min can be noticed. This is first due to the thermal properties calculation. In fact, the advantage of predicting many foods properties with simple formulas for the pure compounds and then applying a mixing rule (always to be verified in a wide range of mixing rules (Carson, 2006)), becomes a disadvantage when compared to specifically measured properties.

Then, the assumption of constant volume can entail several consequences. One of that is the possible movement of the thermocouple, which could have modified the predicted core position. One another consequence is related to the fact that constant volume affect the prediction of density and thermal properties, influencing heat and mass transfer. Anyway, the simulated trend is reasonable (and reasonably general) enough to justify the approach. The experimental trend of the crust temperature is not available. However, the model can predict a reasonable trend, which include, again, a plateau phase and a further increase (as seen in the above-mentioned literature, e.g. (Purlis and Salvadori, 2009a)). This trend is shown in Fig. 8.

5.2. Weight loss

As discussed above, initial and final data on bread weight are available. The model results and the experimental weight data are reported in Fig. 9. The bread water loss, taken into account from the model, are the main responsible for weight loss. From the comparison of the two charts, an initial plateau trend can be evidenced: this respects the initial heating of the bread, when surface temperatures are lower than 100 °C. After that (approximately at 10 min from the baking start), the most important part of the drying process occurs, and weight loss appears to be almost linear till the end of the process.

Comparing the simulation data on weight loss to the experimental ones, the model seems to overestimate the final weight loss. The impact of liquid water diffusion and some other parameters (e.g. heat transport coefficient, bound/free water ratio, etc.) influence both the data and the results, and have to be further investigated. Anyway, a possible interpretation for an overestimated weight loss is that the heat required for drying a porous material (i.e. the latent heat of vaporization to use in the formula) can be higher than that of pure water due to the water–macromolecule interaction (e.g. between water and starch molecules), as found in literature (Wang and Liapis, 2012). In addition, the above-mentioned volume expansion neglect can be, again, responsible for neglected changes in the thermal properties, then influencing the

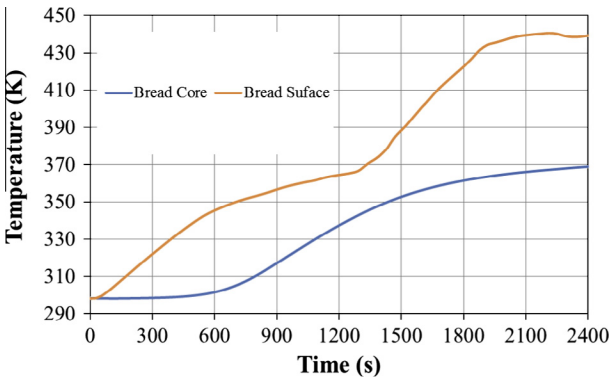

Fig. 8. Simulation, core and surface temperature trends.

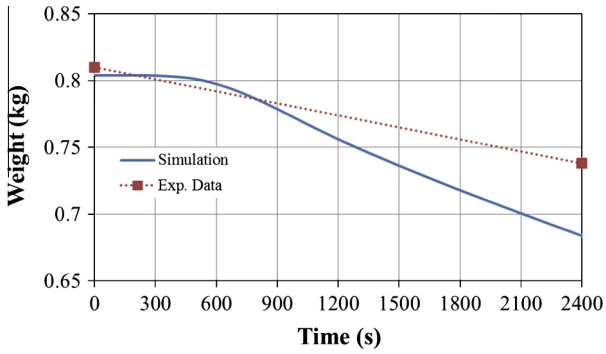

Fig. 9. Weight loss. Model (blue – solid line) and experimental data (red – dotted line) comparison. (For interpretation of the references to color in this figure legend, the reader is referred to the web version of this article.)

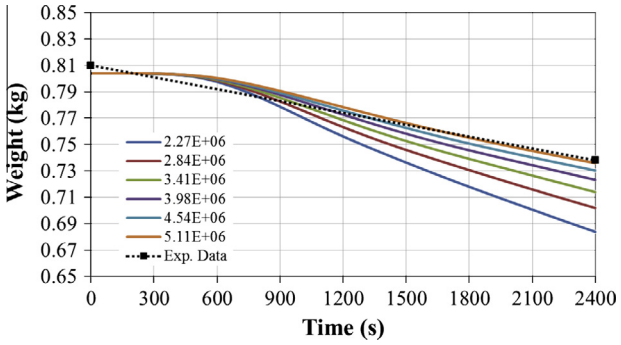

Fig. 10. Weight loss as a function of the latent heat of vaporization.

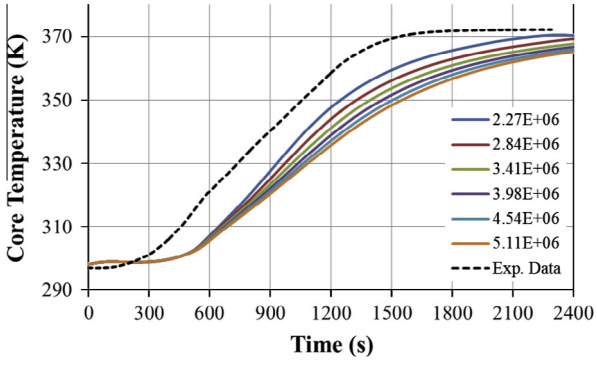

Fig. 11. Core temperature as a function of the latent heat of vaporization.

vaporization ratio prevision. Indeed, volume expansion is related to pore volume increase due to carbon dioxide production and expansion, while the solid phase density can be assumed to be almost constant. According to the change in volume, both density and conductivity of the mixture are modified. In particular, lower conductivity can imply less heat transfer, then less vaporization. At the same time, a longer distance for heat transfer would influence the water vaporization as well, affecting the heat transfer.

5.3. Mesh and computational effort

The physical model is made of 3 highly non-linear partial differential equations in the variables water vapor, liquid water

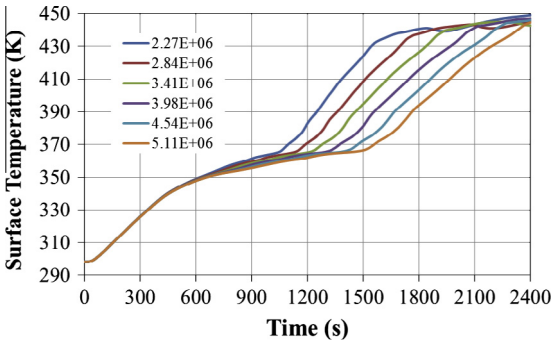

Fig. 12. Crust temperature as a function of the latent heat of vaporization.

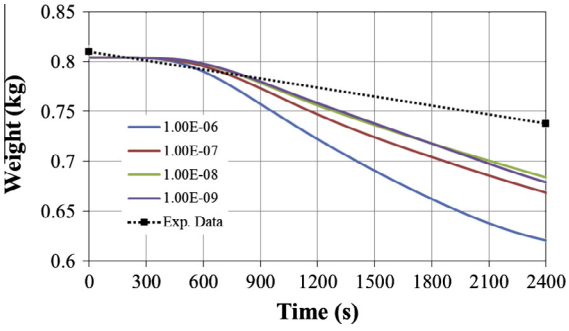

Fig. 13. Weight loss as a function of the liquid water diffusivity.

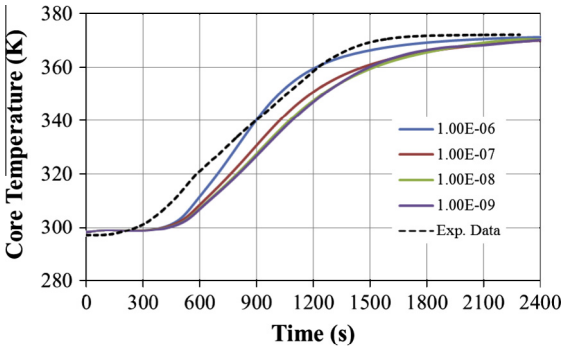

Fig. 14. Core temperature as a function of the liquid water diffusivity.

and temperature. For this reason, a reasonably accurate mesh was chosen, with about 1200 elements and a number of freedom degrees of about 6200. The computational time with an Intel® core7™ i7-3770 processor was about 21 min, reasonable enough to perform sensitivity study without taking a huge time amount. Some parameters have been chosen to be constant in order not to favor further non-linearities in the equations and not to bring to singularity-like behaviors.

6. Conclusions

A model that for the description of bread baking and its temperature and weight loss trends has been implemented, that consists on a coupled PDEs system (energy conservation and water-vapor and liquid-conservation) and has been validated on experimental data (temperature, weight loss). An explicit formulation of water vaporization has been introduced and applied, as never been applied to bread baking. The considered material properties,

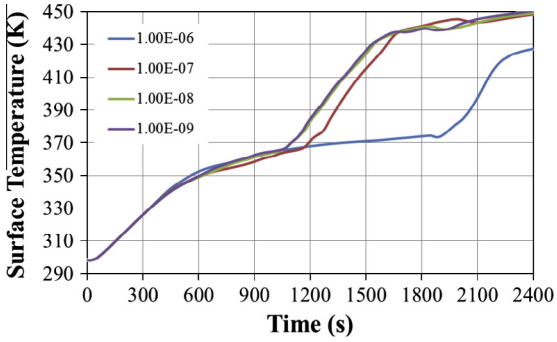

Fig. 15. Crust temperature as a function of the liquid water diffusivity.

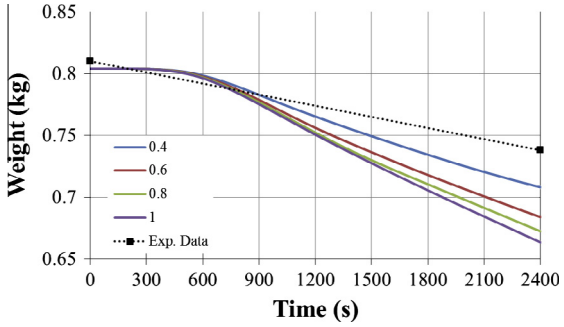

Fig. 16. Weight loss as a function of the initial free water fraction.

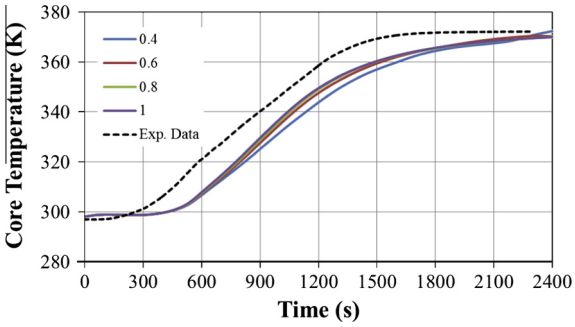

Fig. 17. Core temperature as a function of the initial free water fraction.

depending on the bread macro-components mixture, can permit to represent structural properties variations with bread formulation and to consider the chemical and physical modifications occurring during baking, directly affecting the whole model and giving instruments to control quality issues (e.g. caramelization and Maillard reaction in the crust, starch gelatinization and gluten coagulation in the crumb). A sensitivity analysis on some model parameters has been performed and added as an Appendix A, which confirms a reasonable parameters choice.

Appendix A. Sensitivity analysis

The results show a good qualitative trend of the simulations, despite some differences both in the thermal and in the weight loss can be found. For this reason, a sensitivity analysis has been performed on the achieved solution parameters, in order to understand which of them will require more attention in a future model refinement.

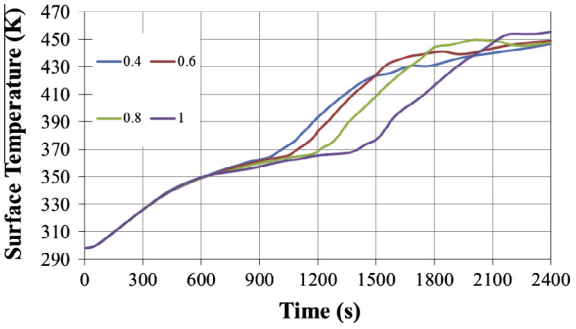

Fig. 18. Surface temperature as a function of the initial free water fraction.

A.1. Sensitivity on the latent heat of vaporization

As told before, a possibility to decrease the drying ratio is that of using a higher heat of vaporization. Increasing that, lower values for weight loss are achieved (Fig. 10), going to the detriment of core temperature fitting (heating delayed, Fig. 11) and less rapid (and thick) crust formation (Fig. 12). Analyzing the results, a reasonable increase of 25% could be a good compromise between the used values. N.B.: The legend reports the heat of vaporization values in J/kg.

A.2. Sensitivity on the liquid water diffusivity

Liquid water diffusion can dominate the vaporization regime, since it influences the availability of the water for the bread surface. The sensitivity analysis show that very low values bring to high weight loss (Fig. 13), to quicker heating of the core due to loss in specific heat associated to water loss (Fig. 14) and slower crust formation, related to the higher liquid water availability in the surface region (Fig. 15).

A.3. Sensitivity on the free water fraction

It is not easy to estimate free and bound water content in food. In case of an evident crust formation, one method could be that of measuring the residual water content in the inner and outer regions and in the raw material, to assume that the crust reached the lower possible value, then deducing the bound water content. Actually, this method is not precise enough, thinking that baking is not a complete drying process. So, a sensitivity analysis on that can be performed to highlight the effects of the free water fraction. N.B.: the legend represents the initial free water fraction related to the total water.

When less water is available to evaporate and diffuse, water loss is unavoidably lower (Fig. 16). In the same time, a not appreciable difference in the core temperature is achieved (Fig. 17), while the crust is created earlier (Fig. 18), bringing to a probable bread surface burning. For this reason, a value between the chosen one (0.6) and the lowest one (0.4) could be fine for simulation.

References

Carson, J.K., 2006. Review of effective thermal conductivity models for foods. Int. J. Refrig. – Revue Internationale Du Froid 29, 958–967.
Chhanwal, N., Indrani, D., Raghavarao, K.S.M.S., Anandharamakrishnan, C., 2011. Computational fluid dynamics modeling of bread baking process. Food Res. Int. 44, 978–983.
Choi, Y., Okos, M.R., 1986. Effects of temperature and composition on the thermal properties of foods. Food Eng. Process Appl. 1, 93–101.
Czuchajowska, Z., Pomeranz, Y., Jeffers, H.C., 1989. Water activity and moisture-content of dough and bread. Cereal Chem. 66, 128–132.
Datta, A.K., van der Sman, R., Gulati, T., Warning, A., 2012. Soft matter approaches as enablers for food macroscale simulation. Faraday Discuss. 158, 435–459.

Della Valle, G., Chiron, H., Cicerelli, L., Kansou, K., Katina, K., Ndiaye, A., Whitworth, M., Poutanen, K., 2014. Basic knowledge models for the design of bread texture. Trends Food Sci. Technol. 36, 5–14.

Dhall, A., Halder, A., Datta, A.K., 2012. Multiphase and multicomponent transport with phase change during meat cooking. J. Food Eng. 113, 299–309.

Gulati, T., Datta, A.K., 2013. Enabling computer-aided food process engineering: property estimation equations for transport phenomena-based models. J. Food Eng. 116, 483–504.

Halder, A., Dhall, A., Datta, A.K., 2011. Modeling transport in porous media with phase change: applications to food processing. J. Heat Transfer – Trans. ASME 133.

Jury, V., Monteau, J.Y., Comiti, J., Le-Bail, A., 2007. Determination and prediction of thermal conductivity of frozen part baked bread during thawing and baking. Food Res. Int. 40, 874–882.

Ni, H., 1997. Multiphase moisture transport in porous media under intensive microwave heating. PhD Thesis, Cornell University.

Nicolas, V., Salagnac, P., Glouannec, P., Ploteau, J.P., Jury, V., Boillereaux, L., 2014. Modelling heat and mass transfer in deformable porous media: application to bread baking. J. Food Eng. 130, 23–35.

Ousegui, A., Moresoli, C., Dostie, M., Marcos, B., 2010. Porous multiphase approach for baking process – explicit formulation of evaporation rate. J. Food Eng. 100, 535–544.

Papasidero, D., Manenti, F., Corbetta, M., Rossi, F., 2014. Relating Bread Baking Process Operating Conditions to the Product Quality: a Modeling Approach. Chem. Eng. Trans. 39, 1729–1734.

Purlis, E., 2012. Baking process design. In: Handbook of Food Process Design. Wiley-Blackwell, Oxford, UK.

Purlis, E., Salvadori, V.O., 2009a. Bread baking as a moving boundary problem. Part 1: Mathematical modelling. J. Food Eng. 91, 428–433.

Purlis, E., Salvadori, V.O., 2009b. Bread baking as a moving boundary problem. Part 2: Model validation and numerical simulation. J. Food Eng. 91, 434–442.

Quang, T.H., Verboven, P., Verlinden, B.E., Herremans, E., Wevers, M., Carmeliet, J., Nicolai, B.M., 2011. A three-dimensional multiscale model for gas exchange in fruit. Plant Physiol. 155, 1158–1168.

Rahman, M.S., Al-Amri, O.S., Al-Bulushi, I.M., 2002. Pores and physico-chemical characteristics of dried tuna produced by different methods of drying. J. Food Eng. 53, 301–313.

Scarpa, F., Milano, G., 2002. The role of adsorption and phase change phenomena in the thermophysical characterization of moist porous materials. Int. J. Thermophys. 23, 1033–1046.

Schirmer, M., Hussein, W.B., Jekle, M., Hussein, M.A., Becker, T., 2011. Impact of air humidity in industrial heating processes on selected quality attributes of bread rolls. J. Food Eng. 105, 647–655.

Wang, J.C., Liapis, A.I., 2012. Water–water and water–macromolecule interactions in food dehydration and the effects of the pore structures of food on the energetics of the interactions. J. Food Eng. 110, 514–524.

Williams, R., Mittal, G.S., 1999. Low-fat fried foods with edible coatings: modeling and simulation. J. Food Sci. 64, 317–322.

Zhang, J., Datta, A.K., 2006. Mathematical modeling of bread baking process. J. Food Eng. 75, 78–89.